

Loss of GLS2 function is essential for obtaining oncogenic functions and promotes the progression of clear cell renal cell carcinoma.

dantong sun

the affiliated hospital of qingdao university

Lu Tian

ocean university of china

Han Zhao

the affiliated hospital of qingdao university

Weihua Yan

the affiliated hospital of qingdao university

Xiaojuan Wei

the affiliated hospital of qingdao university

Yang Wo

the affiliated hospital of qingdao university

helei hou (✉ [houhelei@qdu.edu.cn](mailto:houlhelei@qdu.edu.cn))


the affiliated hospital of qingdao university <https://orcid.org/0000-0001-8502-7461>

Primary research

Keywords: clear cell renal cell carcinoma, renal cell carcinoma, GLS2, E2F, overall survival

Posted Date: February 12th, 2020

DOI: <https://doi.org/10.21203/rs.2.23360/v1>

License:  This work is licensed under a Creative Commons Attribution 4.0 International License. [Read Full License](#)

Abstract

Background

The incidence of RCC has drastically increased in recent years. The large intratumor heterogeneity of RCC, especially ccRCC, usually leads to treatment failure. In addition, single biomarkers have a limited ability to predict prognosis. Therefore, we performed this study to select variables and provided a simple but efficient way to predict prognosis.

Method

Three studies from the GEO database were involved in the selection of DEGs. A total of 840 RCC patients and 524 ccRCC patients from the TCGA database were involved in the prognostic analyses. Nomograms based on the Cox regression model were used to select variables to predict the prognosis, and GSEA was used to demonstrate the potential pathways altered by gene expression.

Result

Our study suggested that DEGs existed between metastatic and primary tumor tissues. Loss of GLS2 function was related to poor prognosis in RCC and ccRCC. These results revealed that GLS2 expression combined with basic characteristics, including age and TNM stage, could efficiently predict prognosis. GLS2 serves as a tumor suppressor in ccRCC, and loss of GLS2 function endows cells with oncogenic functions and is related to advanced disease. According to the GSEA results, loss of GLS2 function may alter the cell cycle by activating the E2F pathway.

Conclusion

GLS2 is a tumor suppressor in RCC. Loss of GLS2 function in ccRCC predicts a poor prognosis via the E2F pathway. Nomograms based on DEGs and clinical features provide doctors with a simple but efficient way to predict prognosis. Further studies are needed to verify the pathway in our study.

Background

Renal cell carcinoma (RCC), which accounts for more than 90% of cancers derived from the kidney [1], has a drastically increasing incidence worldwide in recent years [2], and more than 350,000 patients worldwide are diagnosed with RCC per year [3]. Clear cell RCC (ccRCC), papillary RCC (pRCC) and chromophobe RCC (chRCC) are major subtypes ($\geq 5\%$) that account for approximately 75%, 15% and 5% of RCCs, respectively [1, 4]. RCC has been revealed to be a malignant disease with high heterogeneity, and molecular alterations may play important roles in obtaining oncogenic functions, including invasiveness and the ability to metastasize [5]. In addition to orthodox therapeutics for primary RCC, approved drugs targeting driver genomic alterations for advanced RCC have been widely used [6]. Axitinib [7], sorafenib [8], sunitinib [9, 10], lenvatinib [11] and other approved drugs, such as bevacizumab [12] and immune checkpoint inhibitors (ICIs) [13], provide advanced RCC patients with more options. Unfortunately, the treatment response varies among advanced RCC patients because of tumor heterogeneity, different drug action mechanisms and

varying cancerous biological behaviors [6, 14]. With the development of genomic sequencing, great improvements have been made in precision medicine for RCC in the past decade [6, 15, 16, 17]. Biomarkers for predicting the prognosis of RCC have been detected for clinical use, such as Von Hippel-Lindau tumor suppressor (VHL) and epidermal growth factor receptor (EGFR). However, given that RCC shows great heterogeneity in tumor biological behaviors, the differentially expressed genes (DEGs) in primary and metastatic RCC tissues identified in different studies also show great heterogeneity, and it is difficult to conclude possible biomarkers for predicting the prognosis of RCC.

The Gene Expression Omnibus (GEO) database is a commonly used database for analyses of genomic profiles based on RNA sequencing (RNA-seq) [18]. In our study, we used three previously published studies on the DEGs between primary and metastatic RCC or ccRCC tissues, the RNA-seq data of which can be acquired from the GEO database, including the GSE105261 (ccRCC), GSE47352 (ccRCC) and GSE23629 (RCC) datasets. Seven DEGs (existing in ≥ 2 studies) were detected in our study, and the area under the curve (AUC) of the ROC curves and prognostic nomograms were used for the detection of the most valuable biomarkers for RCC, especially ccRCC. Overall, our study confirmed the important role of glutaminase 2 (GLS2) functional loss in the metastasis of ccRCC and the prognostic value of GLS2 in ccRCC and RCC. In addition, we demonstrated that the E2F pathway was the most likely signaling pathway activated by GLS2 functional loss and that molecules from the E2F family were related to a poor prognosis in ccRCC and RCC.

Methods

Study patients and tissue samples

A total of 840 RCC patients ($n = 840$) and 524 ccRCC patients ($n = 524$) from The Cancer Genome Atlas (TCGA) database were involved in this study for the survival analyses and the construction of prognostic nomograms. Basic information, including age, sex, and TNM stage, was collected for multivariate analysis. Fragments per kilobase of transcript per million fragments mapped (FPKM) values were used for the calculation of RNA expression in this study. This study was approved by the Ethics Committee of the Affiliated Hospital of Qingdao University, and the investigations were carried out following the rules of the Declaration of Helsinki. Thirty primary tumor tissue samples (14 ccRCC samples and 16 RCC samples) and forty-six metastatic tumor tissue samples (30 ccRCC samples and 16 RCC samples) were used for the bioinformatic analyses from the GEO database.

Bioinformatic Analyses

In this study, we used GEO2R online tools to identify DEGs between primary and metastatic tissues. A P value < 0.01 and a ratio of the FPKM values between the two groups (fold change) ≥ 2 were used for the determination of DEGs. DEGs that existed in more than two studies selected from the GEO database were identified as valuable DEGs and used for the next analyses. In addition, the DEGs of each study were subjected to Kyoto Encyclopedia of Genes and Genomes (KEGG) enrichment analyses through DAVID and

KOBAS 3.0 online tools to obtain a comprehensive set of functions of these altered genes. The mutual pathways between the three studies were detected by a Venn plot to identify the most likely pathways altered in metastatic tissues and provide researchers with biological information for further studies. Gene set enrichment analysis (GSEA) was used to confirm the differential signaling pathways and molecules in two sets of patients from the TCGA database grouped by a selected gene. We used OncoLnc [19] and GEPIA [20] to draw Kaplan-Meier plots, and the median expression values of selected genes were used as cutoffs for the univariate analysis. The expression data of selected genes in different samples, TNM stages, metastatic lymph nodes and tumor grades were collected from UALCAN [21].

Statistical Analyses

ROC curves of DEGs and E2F family molecules were generated in this study, and the AUC was used to identify the efficiency in predicting the prognosis of RCC or ccRCC patients. Student's t test was used for the detection of statistical significance in the comparison of gene expression between the group of patients who were alive and the group of patient who had died. Multivariate analysis using the Cox proportional hazard model and a $P < 0.05$ was used to integrate variables into our prognostic nomograms. We used the "rms" package of R software version 3.1.2 (The R Foundation for Statistical Computing, Vienna, Austria) to construct nomograms. Discrimination and calibration were conducted to evaluate the internal validity of nomograms. Harrell's C-indexes ranging from 0.5 (no discrimination) to 1 (perfect discrimination) were used to verify discrimination [22]. Visual calibration plots were used to verify calibration [23]. Bootstrap analyses with 1,000 resamples were used for these analyses. We compared the AUC of each variable with Harrell's C-indexes of the nomograms to determine a better way to predict the prognosis of RCC and ccRCC patients [24]. All figures and statistical processes in our study were performed by R software version 3.1.2 (The R Foundation for Statistical Computing, Vienna, Austria), SPSS 23.0 (SPSS, Inc.) and GraphPad Prisma 8.0 software. P values were two-tailed for all tests, and a $P < 0.05$ was used to define statistical significance.

Results

Identification of DEGs and enrichment analyses

Three studies including GSE105261, GSE47352 and GSE23629 from the GEO database were involved in the analyses. As the volcano plots show in Fig. 1A1-A3, the top 250 DEGs of each study are shown in the plots. DEGs with a fold change ≥ 2 were selected for the next analyses. Seven DEGs identified from more than two studies were finally selected for survival analyses, including GLS2, osteoglycin (OGN), adhesion G protein-coupled receptor F1 (ADGRF1), adaptor-related protein complex 4 epsilon 1 subunit (AP4E1), tetraspanin 3 (TSPAN3), paired-related homeobox 1 (PRRX1) and katanin catalytic subunit A1-like 2 (KATNAL2). The heatmap of the seven DEGs based on 840 RCC patients is shown in Fig. 1B. Among them, KATNAL2 was highly expressed in RCC tissues, and the other DEGs were in low expression states. KEGG enrichment analyses were performed based on all DEGs with fold changes ≥ 2 , and 40 altered pathways were detected, as shown in Fig. 1C. ROC curves of the seven DEGs were constructed, and four DEGs

showed satisfactory AUC values for the prognosis of RCC, including GLS2 (AUC = 0.605, $P < 0.001$), ADGRF1 (AUC = 0.587, $P > 0.001$), KATNAL2 (AUC = 0.595, $P < 0.001$) and OGN (AUC = 0.585, $P < 0.001$), as shown in Fig. 1D1-D4.

Construction of a prognostic nomogram for RCC patients based on DEGs

840 RCC patients and their basic characteristics were obtained from the TCGA database. The mean age of all RCC patients was 60.2 years, ranging from 17 to 90 years. We divided all RCC patients into two groups according to their outcomes, including a group of patients who were alive and a group of patients who died, and compared the expression status of the seven selected DEGs between the two groups, as shown in Figure D5-D8. GLS2, ADGRF1 and KATNAL2 showed a significant reduction in the group of patients who died, which indicated that the functional loss of these genes was associated with a poor prognosis in RCC.

Univariate analyses were performed to demonstrate the relationship between selected DEGs and the prognosis of RCC patients, as shown in Fig. 2A-D. The four selected DEGs were tightly associated with prognosis. High expression of GLS2, ADGRF1 and KATNAL2 was related to a good prognosis both in terms of disease-free survival (DFS) and overall survival (OS). However, high expression of OGN was related to poor DFS and OS. Multivariate analysis was performed to integrate the variables into a nomogram. As shown in Table 1, age ($P = 0.014$), TNM stage ($P < 0.001$) and GLS2 expression ($P = 0.001$) were selected for the nomograms based on multivariate analysis with the Cox regression model. The nomogram for OS of RCC patients was constructed based on the three variables above, as shown in Fig. 2E. In the nomogram, every variable produced a score, and the total score was easy to calculate. By correlating the total score with the 1-year to 5-year OS values, the probability of survival for every patient could be obtained.

Table 1
Univariate and multivariate analyses of RCC patients based on DEGs.

Variables	Groups	Renal cell carcinoma		
		Total Patient (N = 840, x%)	Univariate analysis	Multivariate analysis
age			< 0.001	0.014
	> 60	421(50.1)		
	<=60	419(49.9)		
gender			0.42	0.522
	male	564(67.1)		
	female	276(32.9)		
TNM stage			< 0.001	< 0.001
	I	450(53.6)		
	II-IV	390(46.4)		
GLS2			< 0.001	0.001
	low	420(50.0)		
	high	420(50.0)		
ADGRF1			0.001	0.323
	low	420(50.0)		
	high	420(50.0)		
KATNAL2			< 0.001	0.58
	low	420(50.0)		
	high	420(50.0)		
OGN			0.026	0.349
	low	420(50.0)		
	high	420(50.0)		

The Role Of GLS2 In RCC and ccRCC

The nomogram for the OS of RCC patients revealed that GLS2 plays an important role in the prognosis of RCC. Given that GLS2 was a DEG of the ccRCC samples (GSE105261 and GSE47352), the following analyses were all based on ccRCC samples to reduce the heterogeneity associated with RCC. We first

determined the expression status of GLS2 in ccRCC through immunohistochemistry (IHC) data from the Human Protein Atlas. Strong and weak staining of GLS2 are shown in Fig. 3A. We further researched the expression status of GLS2 in ccRCC samples from the TCGA database, as shown in Fig. 3B-E. Loss of GLS2 expression was likely to induce tumorigenesis. GLS2 expression was lower in tumor tissue than in normal control tissue. In addition, lower GLS2 expression was related to more metastatic lymph nodes, higher TNM stage and higher tumor grade. In ccRCC patients, GLS2 was also a good biomarker for predicting the prognosis in terms of both DFS and OS in ccRCC patients, as shown in Fig. 3F and Fig. 3G, respectively. Therefore, we conducted GSEA to compare the different signaling pathways and molecules between the GLS2-high (GLS2-H) group and GLS2-low (GLS2-L) group. According to the GSEA in this study, the cell cycle pathway was altered significantly in the GLS2-L group according to the results from three pathway databases, as shown in Fig. 3H1-H3, including KEGG (nominal P-value = 0.014), BIOCARTA (nominal P-value = 0.006) and REACTOME (nominal P-value = 0.031). In addition, the E2F pathway (Oncogenic signatures: nominal P-value = 0.006) was overactivated in the GLS2-L group, and E2F1 was overexpressed (Oncogenic signatures: nominal P-value = 0.015; KEGG: nominal P-value = 0.019), as shown in Fig. 4A1-A3.

E2F family and the prognosis of RCC and ccRCC patients

The E2F pathway and molecules of the E2F family were found to be activated in the GLS2-L group of ccRCC patients through GSEA. Therefore, we further determined the relationship between the E2F family and the prognosis of ccRCC and RCC patients. E2F1 to E2F8, which are E2F family molecules detected by researchers so far [25], were included in the prognostic analyses in our study. ROC curves of these eight molecules were constructed in our study, and E2F1, E2F2, E2F3, E2F4, E2F5 and E2F7 showed satisfactory AUC values for predicting the prognosis of ccRCC patients, as shown in Fig. 4B1-B6. Survival analyses for the six selected genes above were performed, and the results are displayed in Fig. 4C1-C6. Except for E2F5, all five other molecules of the E2F family demonstrated a convincing ability to predict the prognosis of ccRCC patients and were all related to poor OS. As a result, we performed multivariate analysis to comprehensively evaluate ccRCC patient prognosis. A total of 524 ccRCC patients from the TCGA database were included in the analysis. The mean age of ccRCC patients was 60.6 years, ranging from 26 to 90 years. Basic characteristics were collected for the construction of a nomogram. Through the multivariate analysis for the OS of ccRCC patients, five variables, including age ($P = 0.001$), TNM stage ($P < 0.001$), E2F1 ($P = 0.037$), E2F4 ($P = 0.012$) and E2F5 ($P = 0.015$), were selected for the construction of a nomogram, as shown in Fig. 5A. The details of the multivariate analysis are summarized in Table 2. Interestingly, although the univariate analysis of E2F5 showed that it had no significance in predicting the prognosis of ccRCC patients, E2F5 may influence prognosis in combination with other factors. E2F1 demonstrated a robust ability to predict the prognosis of ccRCC patients and was activated in the GLS2-L group. We further determined the expression status of E2F1 in the different groups, and the comparisons are shown in Fig. 5B-E. In contrast to that of GLS2, higher E2F1 expression was detected in tumor tissue than in normal tissue, and higher E2F1 expression was related to more metastatic lymph nodes, higher TNM stage and higher tumor grade.

Table 2

Univariate and multivariate analyses of RCC and ccRCC patients based on E2F family members.

variables	groups	Renal cell carcinoma			Clear cell renal cell carcinoma		
		Total Patient, N(%)	Univariate analysis	Multivariate analysis	Total Patient, N(%)	Univariate analysis	Multivariate analysis
age			< 0.001	< 0.001		0.001	0.001
	> 60	421(50.1)			262(50.0)		
	<=60	419(49.9)			262(50.0)		
gender			0.42	0.296		0.695	0.905
	male	564(67.1)			340(64.9)		
	female	276(32.9)			184(35.1)		
TNM stage			< 0.001	< 0.001		< 0.001	< 0.001
	I	450(53.6)			263(50.2)		
	II-IV	390(46.4)			261(49.8)		
GLS2			< 0.001	0.036		NA	NA
	low	420(50.0)			262(50.0)		
	high	420(50.0)			262(50.0)		
E2F1			0.06	0.185		0.001	0.037
	low	420(50.0)			262(50.0)		
	high	420(50.0)			262(50.0)		
E2F2			< 0.001	0.553		0.002	0.884
	low	420(50.0)			262(50.0)		
	high	420(50.0)			262(50.0)		
E2F3			0.008	0.253		< 0.001	0.669
	low	420(50.0)			262(50.0)		
	high	420(50.0)			262(50.0)		
E2F4			NA	NA		< 0.001	0.012
	low	420(50.0)			262(50.0)		

variables	groups	Renal cell carcinoma			Clear cell renal cell carcinoma		
		Total Patient, N(%)	Univariate analysis	Multivariate analysis	Total Patient, N(%)	Univariate analysis	Multivariate analysis
	high	420(50.0)			262(50.0)		
E2F5			NA	NA		0.773	0.015
	low	420(50.0)			262(50.0)		
	high	420(50.0)			262(50.0)		
E2F7			< 0.001	0.021		< 0.001	0.891
	low	420(50.0)			262(50.0)		
	high	420(50.0)			262(50.0)		
E2F8			< 0.001	0.091		0.045	0.218
	low	420(50.0)			262(50.0)		
	high	420(50.0)			262(50.0)		

The ability of GLS2 and the E2F family to predict the prognosis of RCC patients was then estimated. E2F2, E2F3, E2F7 and E2F8 demonstrated satisfactory AUC values, as shown in Table 3, and were convincing biomarkers for predicting the prognosis according to the univariate analyses, the findings of which are summarized in Table 2. Age ($P < 0.001$), TNM stage ($P < 0.001$), GLS2 ($P = 0.036$) and E2F7 ($P = 0.021$) were selected for the construction of a nomogram based on the findings of the multivariate analysis, as shown in Fig. 6A. Given the heterogeneity of RCC, E2F7 is likely to be an important biomarker for prognosis. As shown in Fig. 6B-D, higher expression of E2F7 was detected in the group of RCC patients who died than in the group of RCC patients who were alive, and high expression of E2F7 was related to a poor prognosis in terms of both DFS and OS in RCC patients.

Table 3
The comparison of AUC and C-index.

		Renal cell carcinoma		Clear cell renal cell carcinoma	
		AUC or C-Index	P value	AUC or C-Index	P value
Differential expressed genes	GLS2	0.605	< 0.001	0.605	< 0.001
	KATNAL2	0.595	< 0.001	NA	NA
	ADGRF1	0.587	< 0.001	NA	NA
	OGN	0.585	< 0.001	NA	NA
	PRRX1	0.54	0.076	NA	NA
	AP4E1	0.54	0.076	NA	NA
	TSPAN3	0.526	0.254	NA	NA
E2F FAMILY	E2F1	0.587	0.001	0.581	< 0.001
	E2F2	0.603	< 0.001	0.667	< 0.001
	E2F3	0.603	< 0.001	0.626	< 0.001
	E2F4	0.607	< 0.001	0.524	0.281
	E2F5	0.596	< 0.001	0.566	0.004
	E2F6	0.524	0.375	0.539	0.088
	E2F7	0.608	< 0.001	0.677	< 0.001
	E2F8	0.554	0.046	0.607	< 0.001
Prognostic model	Nomograms	C-Index 1: 0.7790; C-Index 2: 0.7888		C-Index: 0.7679	

Validation of Nomogram Performance

Harrell's C-indexes were calculated to evaluate the discrimination ability of the nomograms and were involved in the comparison of the abilities of the nomograms and other biomarkers in predicting prognosis. The comparisons of AUC values and C-indexes are shown in Table 3. The nomograms demonstrated a more robust ability to predict prognosis than any other single variable selected in this study in RCC patients and ccRCC patients. The calibration plots are shown in Figure S1. The probabilities of our prognostic models agreed with the accuracy probabilities on acceptable scales (dashed lines in the calibration plots correspond to a 10% margin of error) except for that of the 5-year OS model.

Discussion

Glutaminase initiates glutamine catabolism, which is essential for tumorigenesis, and glutaminase is encoded by two genes in mammals, GLS1 and GLS2 [26]. GLS2, which is also called liver-type glutaminase, is primarily expressed in liver, pancreas and brain tissue [27]. Previous studies have proven that GLS2 serves as a tumor suppressor in liver and brain cancer [28, 29]. GLS2 is a target gene of p53 [30] and is related to DNA hypermethylation. In breast cancer, GLS2 expression differs across the luminal subtypes [31], with higher expression of GLS2 in luminal A and B types than in basal-subtype breast cancer. In addition, GLS2 is a druggable metabolic node for breast cancer. In RCC, metabolic reprogramming is closely associated with disease progression and metastasis; as a result, glutaminase inhibitors are a novel strategy for RCC treatment [32]. Although GLS2 is predominantly found in liver tissue, its function as a tumor suppressor in RCC requires further discussion.

In this study, we estimated the relationship between GLS2 and the prognosis of RCC and ccRCC patients and revealed that GLS2 serves as a tumor suppressor in renal cancer. Low GLS2 expression was associated with a poor prognosis in RCC and ccRCC patients and a significant tumorigenesis tendency. We found that low GLS2 expression endowed ccRCC cells with invasiveness and the ability to metastasize because patients with lower GLS2 expression had a worse TNM stage than those with higher GLS2 expression. In addition, low GLS2 expression also increased the malignant degree of ccRCCs, which participated in its ability to predict prognosis in ccRCC. Our prognostic nomogram confirmed the tumor suppressor function of GLS2.

GSEA demonstrated that the E2F pathway was a potential signaling pathway activated by low GLS2 expression. Previous studies confirmed that the E2F pathway controlled tumor cell growth [33, 34] by influencing cell cycle transition and DNA replication. Eight molecules of the E2F family, including E2F1 to E2F8, play different roles in this pathway as a result of their different molecular structures, which are caused by various combinations of pocket proteins [35]. Among E2F family members, E2F1, E2F2 and E2F3 are activators, while E2F4, E2F5 and E2F6 are repressors. Although the tumorigenesis-inducing effect of the E2F pathway is known [36], the role of each E2F family member and the interaction between members in carcinogenesis and cancerous progression remain unclear. In our study, we estimated the prognostic ability of all molecules from the E2F family by univariate and multivariate analyses. For ccRCC patients, most of the E2F family members were related to a poor prognosis, especially E2F1, E2F4 and E2F5, according to our nomogram based on the results of the Cox regression model. The integrated influence of E2F1, E2F4 and E2F5 on clinical characteristics, including age and TNM stage, eventually changes the outcome of ccRCC patients. However, E2F7 is the most important E2F family member in RCC patients according to the nomogram, which is different from that in ccRCC patients.

Substantial heterogeneity was detected in ccRCC tissues in previous studies, and single biomarkers or biomarkers for predicting prognosis concluded from studies with fewer samples usually cannot meet the standard of efficacy and lead to treatment failure [37, 38]. RNA-seq data from three studies were included in this study to overcome the heterogeneity, as identifying DEGs between primary and metastatic tissues would represent the prognosis better than target sequencing of single tissue. In addition, we constructed

nomograms based on the Cox regression model to offer a simple and efficient method for prognostic evaluation. Clinical characteristics and genomic signatures were all involved in the construction of a prognostic model based on a nomogram, which would better discriminate the different prognoses of patients than the previously identified single biomarkers.

Admittedly, some limitations exist in our study. As shown in calibration plots, the ability of our prognostic models to predict the 5-year OS of both ccRCC and RCC patients is not satisfactory. This shortcoming is related to unknown genetic alterations that may occur during the development of renal cancer that cannot be predicted by the signatures and clinical characteristics at first diagnosis of the disease. Dynamic sequencing for patients is a necessity in the treatment of the disease. In addition, further in vitro experiments are needed to verify the relationship between GLS2 functional loss and the activation of the E2F pathway.

Conclusion

In conclusion, GLS2 serves as a tumor suppressor in ccRCC, and loss of GLS2 function is related to poor prognosis. GSEA suggested that the E2F pathway may be activated by loss of GLS2 function. E2F1, E2F4 and E2F5 influence the prognosis of ccRCC patients together with age and TNM stage, while E2F7 is the key influencer of the E2F family, being associated with the prognosis of RCC patients. We constructed nomograms to display our results and offer a simple but efficient method to evaluate the prognosis of ccRCC and RCC patients. Further research is needed to verify our results.

Abbreviations

Renal cell carcinoma (RCC)

Clear cell RCC (ccRCC)

Chromophobe RCC (chRCC)

Immune checkpoint inhibitors (ICIs)

Von Hippel-Lindau tumor suppressor (VHL)

Epidermal growth factor receptor (EGFR)

Differentially expressed genes (DEGs)

Gene Expression Omnibus (GEO)

RNA sequencing (RNA-seq)

Glutaminase 2 (GLS2)

Fragments per kilobase of transcript per million fragments mapped (FPKM)

Gene Set Enrichment Analysis (GSEA)

Osteoglycin (OGN)

Adhesion G protein-coupled receptor F1 (ADGRF1)

Adaptor-related protein complex 4 epsilon 1 subunit (AP4E1)

Tetraspanin 3 (TSPAN3)

Paired-related homeobox 1 (PRRX1)

Katanin catalytic subunit A1-like 2 (KATNAL2)

Disease-free survival (DFS)

Overall survival (OS)

Area under the curve (AUC)

Declarations

-Ethics approval and consent to participate

Not applicable

-Consent for publication

The article was approved by all authors for publication

-Availability of data and material

The data used during the current study is available from the corresponding author on reasonable request.

-Competing interests

The authors declared no conflicts on interests.

-Funding

Special Funding for Qilu Sanitation and Health Leading Talents Cultivation Project (to Helei Hou)

-Authors' contributions

Conception/design: Helei Hou and Dantong Sun;

Collection and/or assembly of data: Dantong Sun, Lu Tian and Xiaojuan Wei;

Data analysis and interpretation: Dantong Sun, Lu Tian and Xiaojuan Wei;

Manuscript writing: Helei Hou and Dantong Sun;

Final approval of the manuscript: All authors.

-Acknowledgments

Our work was supported by Special Funding for Qilu Sanitation and Health Leading Talents Cultivation Project to Helei Hou.

References

1. Hsieh JJ, Purdue MP, Signoretti S, et al. Renal cell carcinoma. *Nat Rev Dis Primers*. 2017, 3: 17009.
2. Capitanio U, Montorsi F. Renal cancer. *Lancet*. 2016, 387(10021): 894-906.
3. Ferlay JSI, Ervik M, Dikshit R, et al. GLOBOCAN 2012 v1.0, cancer incidence and mortality worldwide: IARC CancerBase No. 11. 2013. <http://globocan.iarc.fr> (accessed Jan 1, 2015).
4. Moch H, Cubilla AL, Humphrey PA, et al. The 2016 WHO classification of tumours of the urinary system and male genital organs-part A: renal, penile, and testicular tumours. *Eur Urol*. 2016, 70: 93-105.
5. Shuch B, Amin A, Armstrong AJ, et al. Understanding pathologic variants of renal cell carcinoma: distilling therapeutic opportunities from biologic complexity. *Eur Urol*. 2015, 67: 85-97.
6. Hsieh JJ, Le V, Cao D, et al. Genomic classifications of renal cell carcinoma: a critical step towards the future application of personalized kidney cancer care with pan-omics precision. *J Pathol*. 2018, 244(5): 525-537.
7. Rini BI, Plimack ER, Stus V, et al. Pembrolizumab plus Axitinib versus Sunitinib for Advanced Renal-Cell Carcinoma. *N Engl J Med*. 2019, 380(12): 1116-1127.
8. Haas NB, Manola J, Uzzo RG, et al. Adjuvant sunitinib or sorafenib for high-risk, non-metastatic renal-cell carcinoma (ECOG-ACRIN E2805): a double-blind, placebo-controlled, randomised, phase 3 trial. *Lancet*. 2016, 387(10032): 2008-2016.
9. Jonasch E, Slack RS, Geynisman DM, et al. Phase II Study of Two Weeks on, One Week off Sunitinib Scheduling in Patients With Metastatic Renal Cell Carcinoma. *J Clin Oncol*. 2018, 36(16): 1588-1593.
10. Méjean A, Ravaud A, Thezenas S, et al. Sunitinib Alone or after Nephrectomy in Metastatic Renal-Cell Carcinoma. *N Engl J Med*. 2018, 379(5): 417-427.
11. Motzer RJ, Hutson TE, Glen H, et al. Lenvatinib, everolimus, and the combination in patients with metastatic renal cell carcinoma: a randomised, phase 2, open-label, multicentre trial. *Lancet Oncol*. 2015, 16(15): 1473-1482.
12. Flaherty KT, Manola JB, Pins M, et al. BEST: A Randomized Phase II Study of Vascular Endothelial Growth Factor, RAF Kinase, and Mammalian Target of Rapamycin Combination Targeted Therapy With Bevacizumab, Sorafenib, and Temsirolimus in Advanced Renal Cell Carcinoma—A Trial of the ECOG-ACRIN Cancer Research Group (E2804). *J Clin Oncol*. 2015, 33(21): 2384-2391.

13. Escudier B, Motzer RJ, Sharma P, et al. Treatment Beyond Progression in Patients with Advanced Renal Cell Carcinoma Treated with Nivolumab in CheckMate 025. *Eur Urol*. 2017, 72(3): 368-376.
14. Hsieh JJ, Manley BJ, Khan N, et al. Overcome tumor heterogeneity-imposed therapeutic barriers through convergent genomic biomarker discovery: a braided cancer river model of kidney cancer. *Semin Cell Dev Biol*. 2017, 64: 98-106.
15. Voss MH, Reising A, Cheng Y, et al. Genomically annotated risk model for advanced renal-cell carcinoma: a retrospective cohort study. *Lancet Oncol*. 2018, 19(12): 1688-1698.
16. Pal SK, Ali SM, Yakirevich E, et al. Characterization of Clinical Cases of Advanced Papillary Renal Cell Carcinoma via Comprehensive Genomic Profiling. *Eur Urol*. 2018, 73(1): 71-78.
17. Riazalhosseini Y, Lathrop M. Precision medicine from the renal cancer genome. *Nat Rev Nephrol*. 2016, 12(11): 655-666.
18. Wang C, Gong B, Bushel PR, et al. The concordance between RNA-seq and microarray data depends on chemical treatment and transcript abundance. *Nat Biotechnol*. 2014, 32(9): 926-932.
19. Anaya J. OncoLnc: linking TCGA survival data to mRNAs, miRNAs, and lncRNAs. *PeerJ Computer Science*. 2016, 2:e67.
20. Tang Z, Li C, Kang B, et al. GEPIA: a web server for cancer and normal gene expression profiling and interactive analyses. *Nucleic Acids Res*. 2017, 45(W1): W98-W102.
21. Chandrashekar DS, Bashel B, Balasubramanya SAH, et al. UALCAN: A portal for facilitating tumor subgroup gene expression and survival analyses. *Neoplasia*. 2017, 19(8): 649-658.
22. Bandos AI, Rockette HE, Song T, et al. Area under the free-response ROC curve (FROC) and a related summary index. *Biometrics*. 2009, 65(1): 247-256.
23. Jin C, Cao J, Cai Y, et al. A nomogram for predicting the risk of invasive pulmonary adenocarcinoma for patients with solitary peripheral subsolid nodules. *J Thorac Cardiovasc Surg*. 2017, 153(2): 462-469.
24. Kim SY, Yoon MJ, Park YI, et al. Nomograms predicting survival of patients with unresectable or metastatic gastric cancer who receive combination cytotoxic chemotherapy as first-line treatment. *Gastric Cancer*. 2018, 21(3): 453-463.
25. DeGregori J, Johnson DG. Distinct and Overlapping Roles for E2F Family Members in Transcription, Proliferation and Apoptosis. *Curr Mol Med*. 2006, 6(7): 739-748.
26. Katt WP, Lukey MJ, Cerione RA. A tale of two glutaminases: homologous enzymes with distinct roles in tumorigenesis. *Future Med Chem*. 2017, 9(2): 223-243.
27. Altman BJ, Stine ZE, Dang CV. From Krebs to clinic: glutamine metabolism to cancer therapy. *Nat Rev Cancer*. 2016, 16(10): 619-634.
28. Matés JM, Campos-Sandoval JA, Márquez J. Glutaminase isoenzymes in the metabolic therapy of cancer. *Biochim Biophys Acta Rev Cancer*. 2018, 1870(2): 158-164.
29. Szeliga M, Bogacińska-Karaś M, Kuźmicz K, et al. Downregulation of GLS2 in glioblastoma cells is related to DNA hypermethylation but not to the p53 status. *Mol Carcinog*. 2016, 55(9): 1309-1316.

30. Hu W, Zhang C, Wu R, et al. Glutaminase 2, a novel p53 target gene regulating energy metabolism and antioxidant function. *Proc Natl Acad Sci U S A*. 2010, 107(16): 7455-7460.
31. Lukey MJ, Cluntun AA, Katt WP, et al. Liver-Type Glutaminase GLS2 Is a Druggable Metabolic Node in Luminal-Subtype Breast Cancer. *Cell Rep*. 2019, 29(1): 76-88.
32. Hoerner CR, Chen VJ, Fan AC. The 'Achilles Heel' of Metabolism in Renal Cell Carcinoma: Glutaminase Inhibition as a Rational Treatment Strategy. *Kidney Cancer*. 2019, 3(1): 15-29.
33. Lasham A, Samuel W, Cao H, et al. YB-1, the E2F pathway, and regulation of tumor cell growth. *J Natl Cancer Inst*. 2012, 104(2): 133-146.
34. Hayami S, Yoshimatsu M, Veerakumarasivam A, et al. Overexpression of the JmJc histone demethylase KDM5B in human carcinogenesis: involvement in the proliferation of cancer cells through the E2F/RB pathway. *Mol Cancer*. 2010, 9: 59.
35. Cam H, Dynlacht BD. Emerging roles for E2F: beyond the G1/S transition and DNA replication. *Cancer Cell*. 2003, 3(4): 311-316.
36. Chen HZ, Tsai SY, Leone G. Emerging roles of E2Fs in cancer: an exit from cell cycle control. *Nat Rev Cancer*. 2009, 9(11): 785-797.
37. Serie DJ, Joseph RW, Cheville JC, et al. Clear Cell Type A and B Molecular Subtypes in Metastatic Clear Cell Renal Cell Carcinoma: Tumor Heterogeneity and Aggressiveness. *Eur Urol*. 2017, 71(6): 979-985.
38. Gerlinger M, Rowan AJ, Horswell S, et al. Intratumor heterogeneity and branched evolution revealed by multiregion sequencing. *N Engl J Med*. 2012, 366(10): 883-892.

Figures

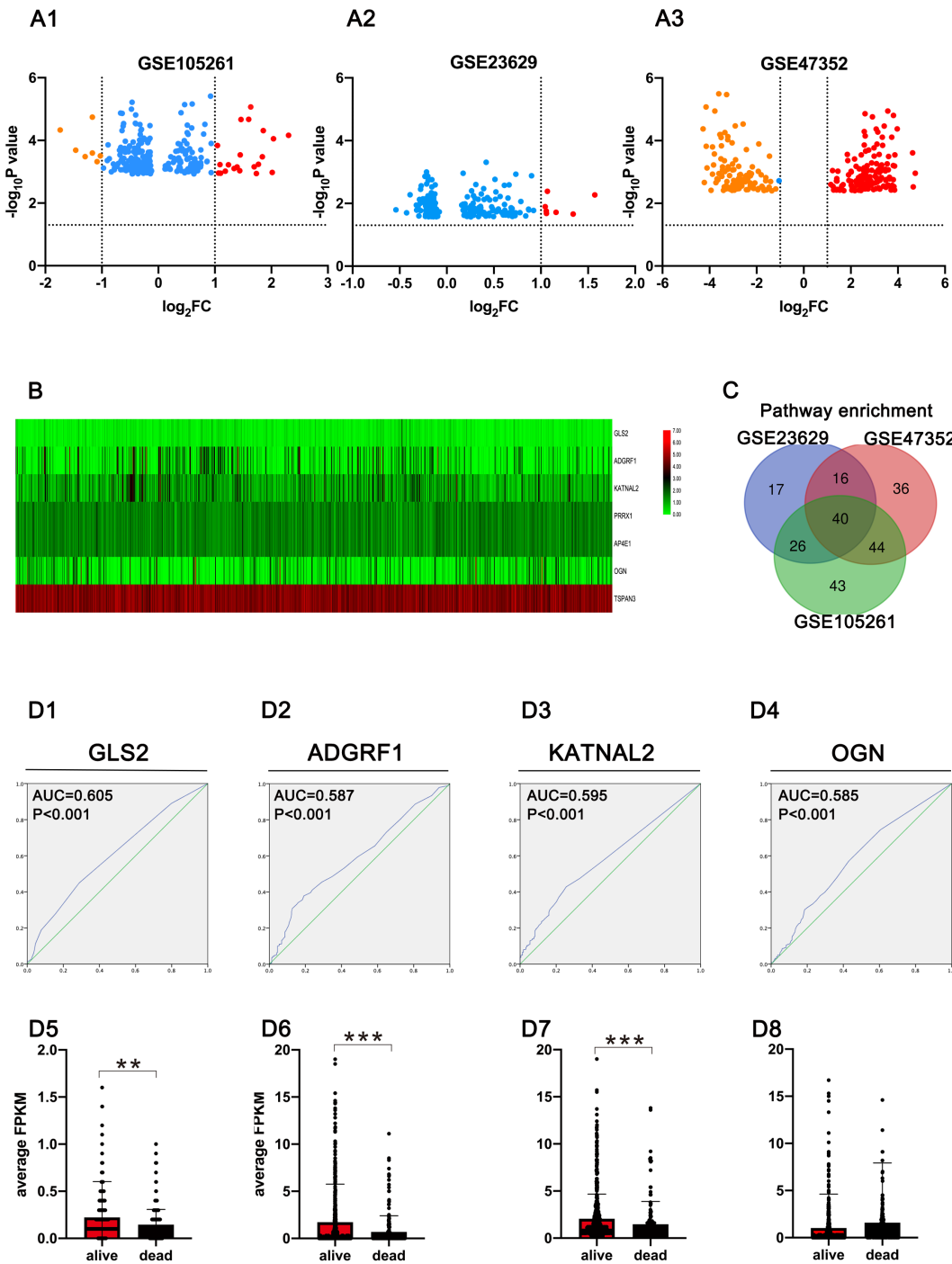


Figure 1

The selection of DEGs. A1: volcano plot of GSE105261; A2: volcano plot of GSE23629; A3: volcano plot of GSE47352; B: heatmap of DEGs; C: Venn plot for pathways of enrichment analyses; D1-D4: ROC curves of selected DEGs with satisfied AUC; D5-D8: comparison of DEGs expression between alive and dead patients.

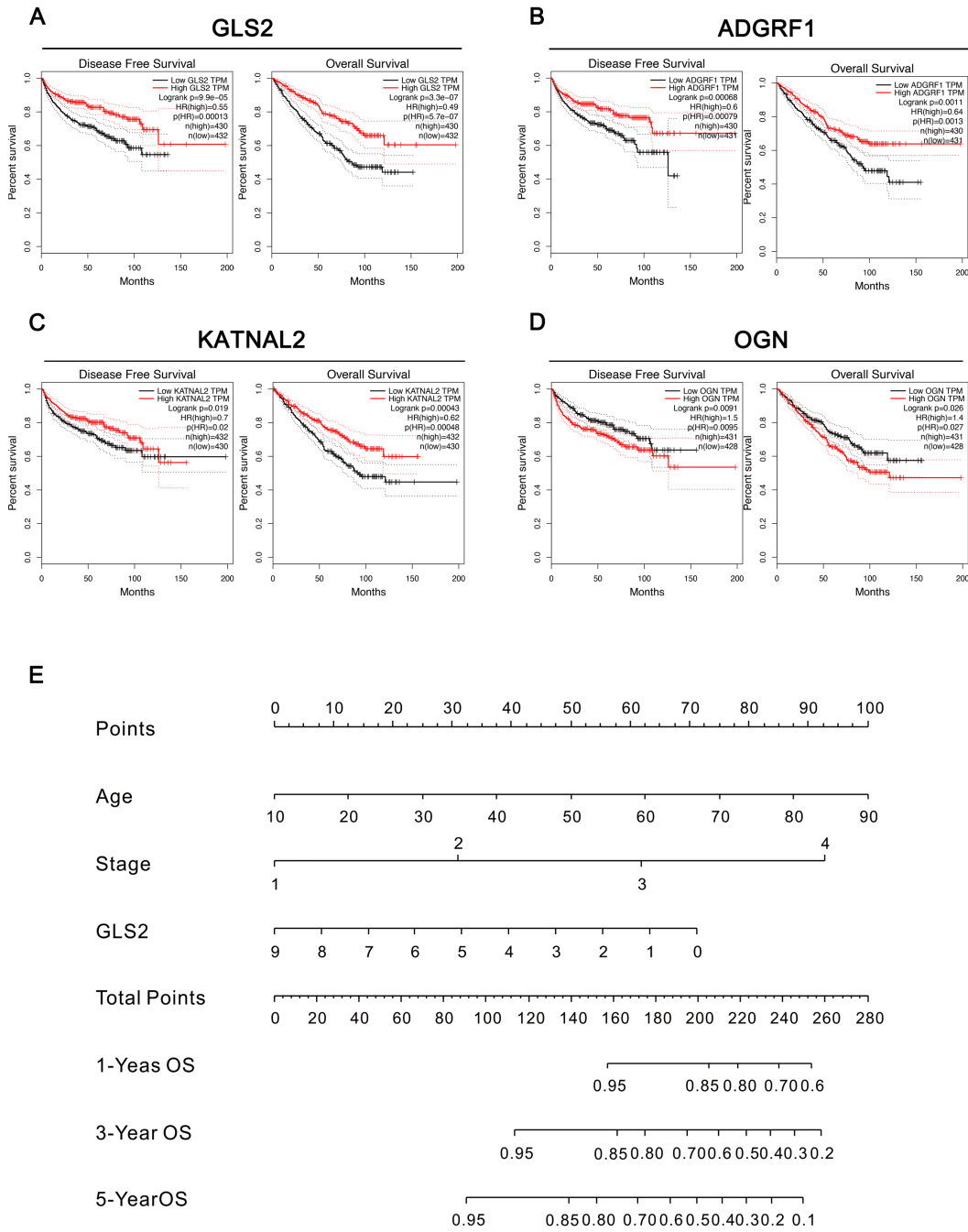


Figure 2

Univariate and multivariate analyses of DEGs in RCC patients. A-D: univariate analyses of DEGs in DFS and OS among RCC patients; E: nomogram based on COX regression model for RCC patients.

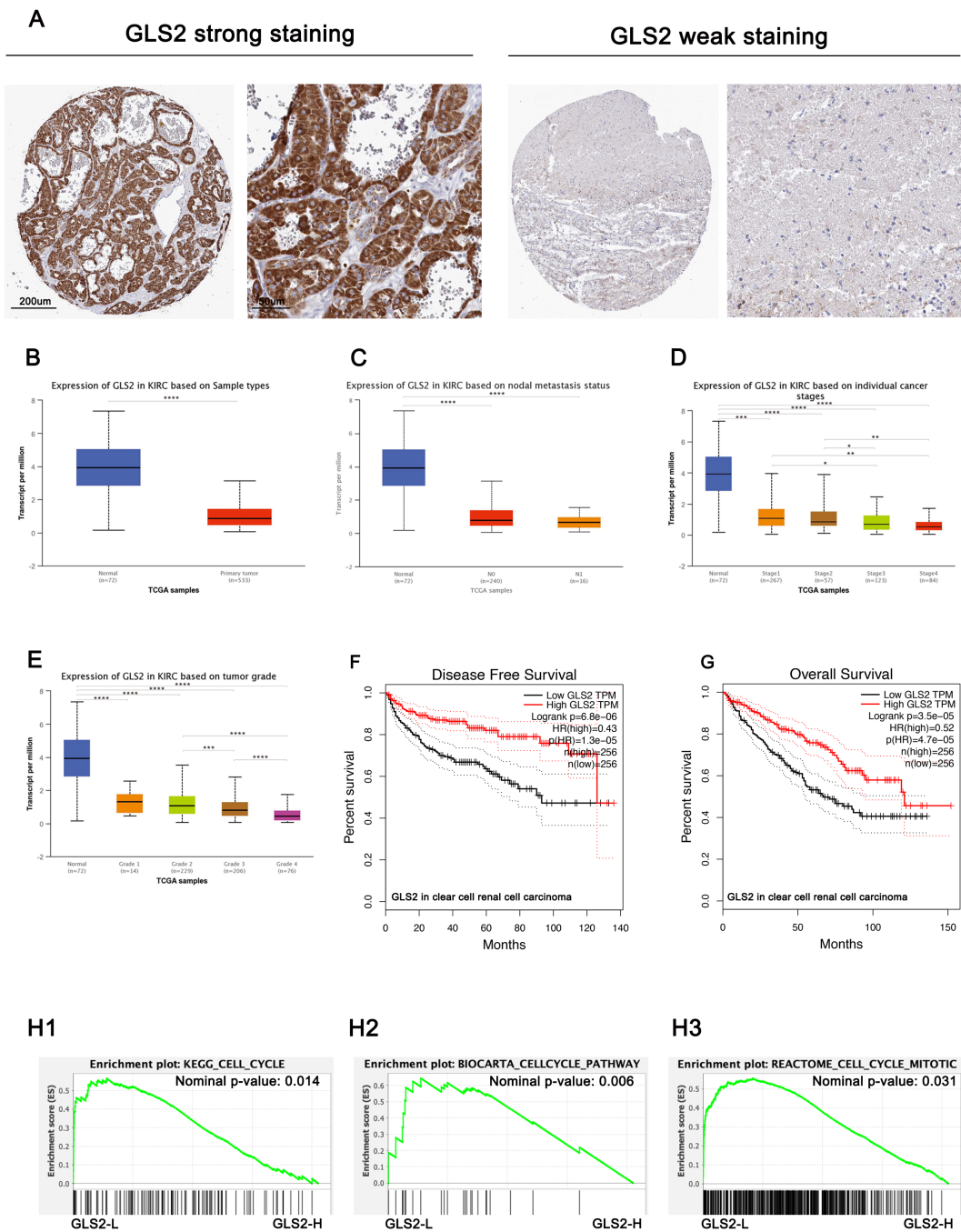


Figure 3

The role of GLS2 in ccRCC patients. A: the IHC images of GLS2 in ccRCC; B: the expression of GLS2 in ccRCC based on sample types; C: the expression of GLS2 in ccRCC based on nodal metastasis status; D: the expression of GLS2 in ccRCC based on individual cancer stages; E: the expression of GLS2 in ccRCC based on tumor grade; F: DFS of ccRCC grouped by GLS2 expression; G: OS of ccRCC grouped by GLS2 expression; H1-H3: GSEA analyses in ccRCC patients grouped by GLS2 expression.

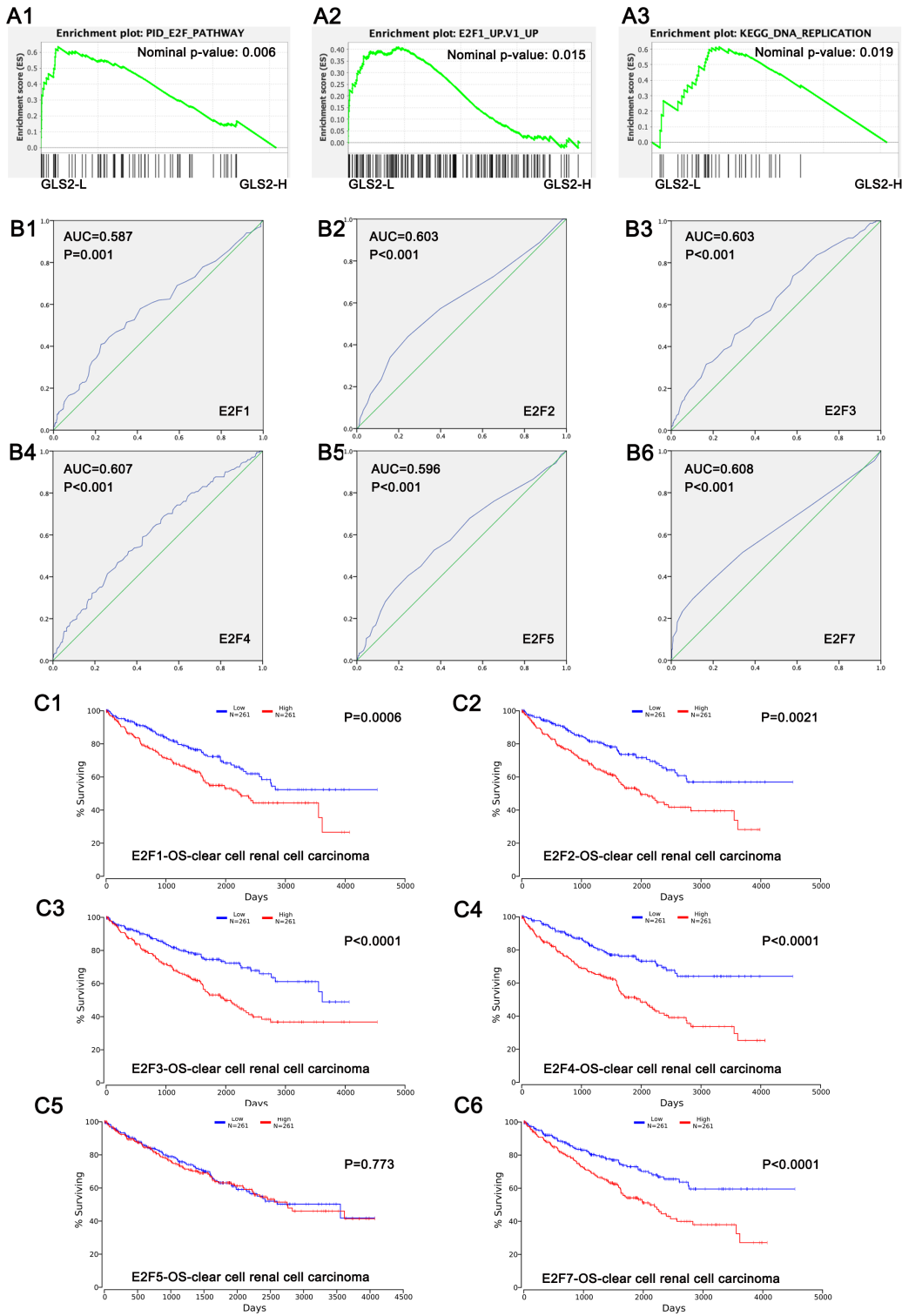


Figure 4

The role E2F family in ccRCC patients. A1-A3: GSEA analyses in ccRCC patients based on GLS2 expression; B1-B6: ROC curves of E2F family members with satisfied AUC; C1-C6: OS of ccRCC patients grouped by E2F family members.

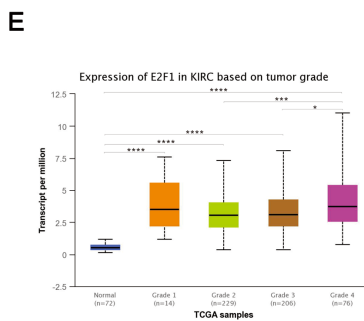
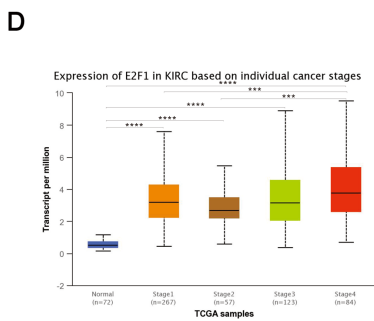
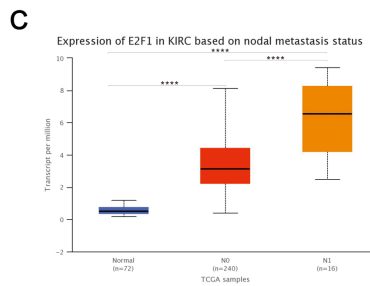
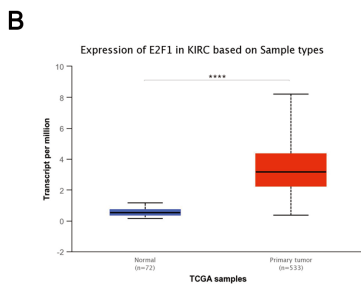
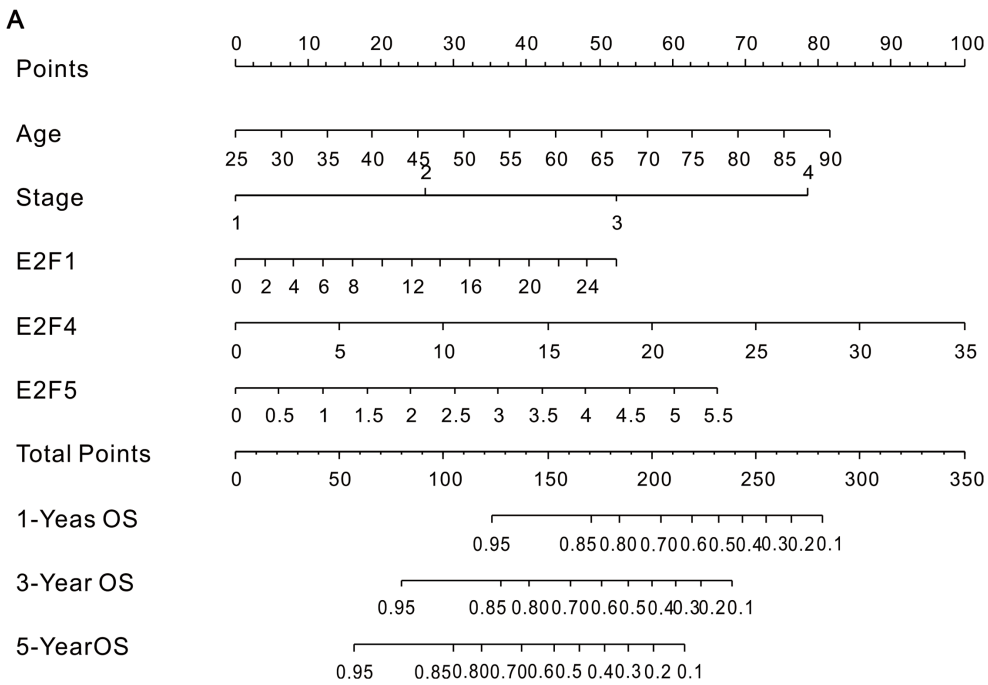


Figure 5

The relationship between E2F family members and ccRCC prognosis. A: nomogram for ccRCC patients based on COX regression model; B: the expression of E2F1 in ccRCC based on sample types; C: the expression of E2F1 in ccRCC based on nodal metastasis status; D: the expression of E2F1 in ccRCC based on individual cancer stages; E: the expression of E2F1 in ccRCC based on tumor grade;

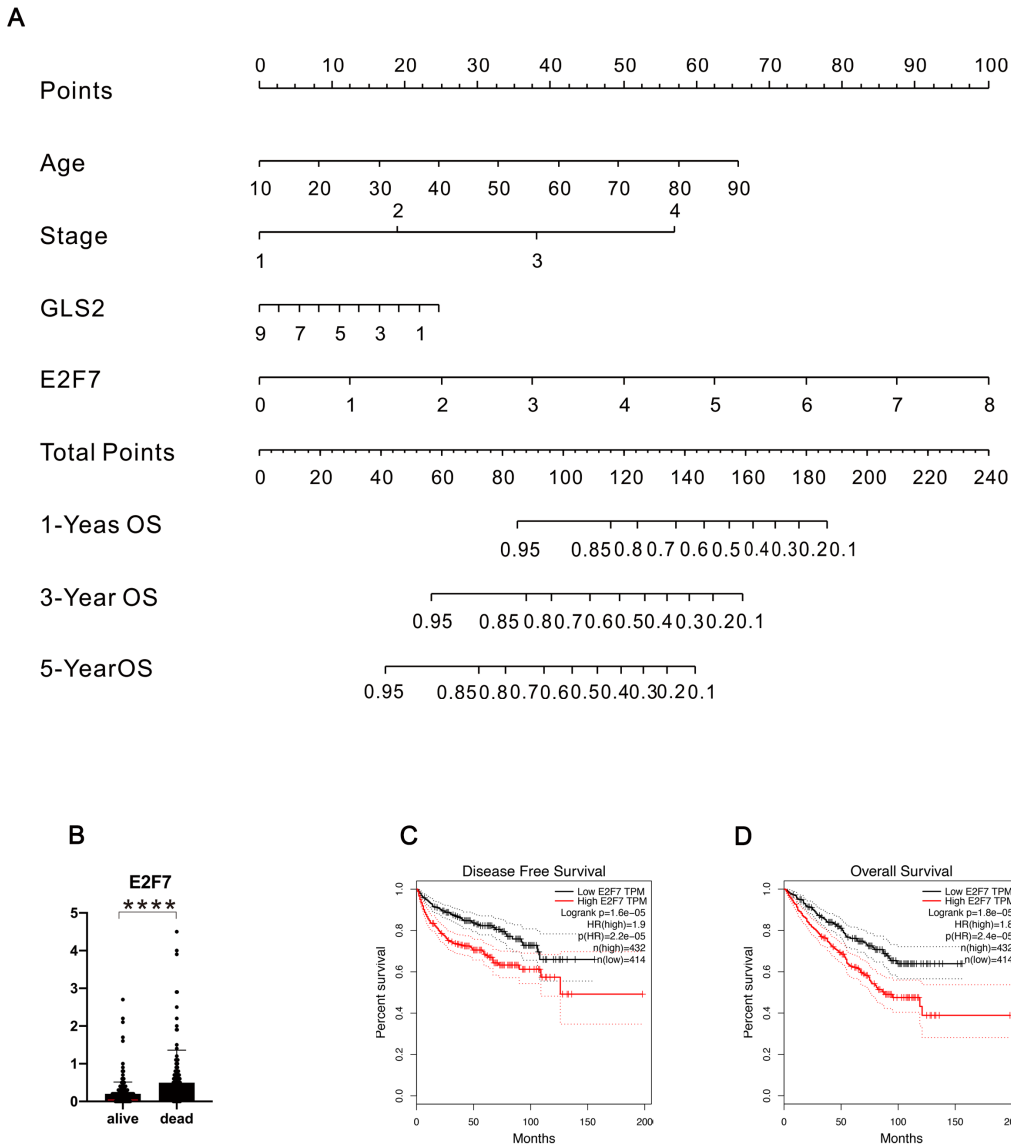


Figure 6

The relationship between E2F family members and RCC prognosis. A: nomograms for RCC patients based on COX regression model; B: the expression of E2F7 in alive and dead patients; C: DFS of RCC patients grouped by E2F7 expression; D: OS of RCC patients grouped by E2F7 expression.

Supplementary Files

This is a list of supplementary files associated with this preprint. Click to download.

- [supplementaryfigureS1.docx](#)